Characterization and Sinterability of Oxide-Dispersion Strengthened Nickel Powder Produced by Mechanical Alloying

K.E. Mohamed, H.P. Buchkremer, and D. Stover

Among the main requirements for the Ni/8% yttria stabilized zirconia (Ni/8YSZ) material, currently used for manufacturing solid oxide fuel cell (SOFC) anodes, fine homogeneous microstructure, considerable structural and mechanical stability, and sufficient gas permeability are of primary concern. In the present investigation, oxide-dispersion strengthened composite Ni powders containing 2, 5, and 10 vol.% 8YSZ were produced by mechanical alloying (MA) in air using a planetary milling machine and ZrO_2 milling media. The progress of the MA process was followed by particle size analysis, optical metallography, and x-ray diffraction (XRD) techniques. Results showed that dispersion of the oxide particles and structural refinement reached a significant point after milling for 180 h. The crystallite size and lattice distortion showed considerable dependence on the processing parameters. The mechanically alloyed powders were sintered at 1100° to 1350 °C. The mechanically alloyed powder containing 10 vol.% 8YSZ exhibited maximum densification. The minimum sintered density was observed for the composite powder containing 2 vol.% 8YSZ.

1. Introduction

In the last two decades, mechanical alloying (MA) has attracted the attention of many investigators as a tool for processing a wide range of materials, which are difficult or entirely impossible to produce by conventional production methods. It has been applied to the production of dispersion-strengthened alloys for high-temperature applications,[1] alloys of very limited solid solubility such as Fe-Cu alloys,[2] intermetallic phases,[3,4] amorphous alloys,[3,5–7] and quasicrystalline and nanocrystalline materials,[8,9] as well as to the production of stabilized zirconia by other oxide additions.[10] The present work reports on the application of MA for the production of composite powders consisting of Ni and zirconia partially stabilized by 8 mol.% Y_2O_3. Hereafter, this powder is referred to as Ni/8YSZ. This system is investigated as a potential candidate material for solid oxide fuel cell (SOFC) anode manufacturing.

At the present time, SOFC anodes are manufactured from a mixture of Ni and 8YSZ powders sintered to a continuous porous structure. In addition to electronic conductivity and other physical properties, the anode material must have long-term microstructural stability and sufficient gas permeability at the SOFC operating conditions. Normally, the SOFC energy systems are operated under oxidizing/reducing atmosphere in the temperature range of 850 to 1050 °C using H_2 or CO as a fuel and producing H_2O or CO_2 as a reaction product. In a previous investigation, however, it was shown that the electrochemical performance of the anode manufactured by sintering of simply mixed Ni/8YSZ powder is deteriorated with time under SOFC operating conditions.[11] This was attributed to grain coarsening of the Ni matrix of the anode.

Dispersion of fine, inert stable particles in metal powders has been found to slow down or inhibit sintering of the metal powders containing them. Such particles include oxides, refractory metals, graphite, and possible spinel oxides. This inhibiting effect was reviewed and discussed by Ashby *et al.*[12] It was reported that this inhibiting effect increased with dispersoid content until a critical concentration was reached, above which an increase in sinterability was observed. Although there are some investigations reviewed by Ashby *et al.* about the effect of dispersed particles on the sinterability of some metal powders, these studies have only treated the problem for simply mixed powders. Little work has been conducted to study the sinterability of mechanically alloyed metal powders with some oxides.[13,14] However, no systematic investigation was carried out to study the sintering behavior of mechanically alloyed nickel powder with different amounts of oxide dispersoids. Therefore, the aim of the present investigation was to study the effect of MA time on the characteristics of the composite powder Ni/8YSZ for different volume fractions of 8YSZ and to evaluate the sinterability and microstructural changes for compacts of these composite powders after sintering at high temperatures in a reducing atmosphere. The dispersoid content range is 0 to 10 vol.%, which is typically the focus of interest for sinterability studies.

2. Experimental Work

The starting materials were nickel powder from Merck (Darmstadt, Germany), of 99.5% purity with an average particle

K.E. Mohamed, Metallurgy Department, Atomic Energy Authority, 13759 Cairo, Egypt; and **H.P. Buchkremer** and **D. Stover**, Institute for Materials in Energy Systems, Forschungszentrum Jülich, D-52425 Jülich, Germany.

size (d_{50}) of 11.38 μm, and 8 mol.% Y_2O_3 partially stabilized zirconia (8YSZ) from Tosoh Corporation (Tokyo, Japan, TZ-8Y), with an average particle size of 0.3 μm. Powder mixtures consisting of Ni and 0, 2, 5, and 10 vol.% 8YSZ were prepared by mixing Ni with the appropriate amount of 8YSZ for about 24 h. Each powder mixture was charged into a zirconia milling vial with zirconia milling balls of 10 mm diameter. The ball:powder weight ratio was 10:1. For MA, the charged vials were fixed in a high energy planetary milling machine (PM-4, Retsch, Haan, Germany) rotating at a speed of 150 rpm to a maximum MA time of 180 h. Nickel without addition of 8YSZ was also mechanically alloyed under the same conditions as a reference material.

To follow the progress of the MA procedure, powder samples were taken from each powder charge after different milling time intervals for characterization. A laser light diffraction granulometer was used to analyze the particle size of the powder. After certain processing time intervals, the phase composition of the powder was identified by x-ray diffraction (XRD) using Cu K_α radiation (Siemens D 5000, Siemens, Karlsruhe, Germany). Peak broadening of Ni peaks at half-peak intensity was also measured using computer software "DIFFRAC-AT, Siemens."

Green compacts from each powder mixture mechanically alloyed for 90 and 180 h were prepared by uniaxial cold pressing at 600 MPa. The green density of the compacts ranged from 52 to 55% of theoretical. Some of these compacts were sintered at 1100 or 1350 °C for 1 h, while other groups of the compacts were subjected to long-term annealing treatment at 1100 °C for up to 800 h. Both treatments were carried out in a reducing atmosphere consisting of Ar + 4 vol.% H_2. Optical metallography of etched powder samples was conducted to study the microstructural changes during the MA process. The microstructure and porosity of the sintered specimens were also investigated by the same technique. Quantitative evaluation of the porosity distribution was conducted on some sintered samples using a mercury porosimetry method.

Scanning electron microscopy (SEM) examinations of some specimens were made; the x-ray images of Zr and Ni were used to determine the spatial distribution of these elements.

3. Results and Discussion

3.1 Characteristics of the MA Powders

Figure 1 presents the relationship between the milling time and the particle size of the Ni/8YSZ powders. It clearly indicates predomination of the welding process of Ni particles in the early stages of MA due to its remarkable ductility. As a result, all the powder particle size fractions d_{10}, d_{50}, and d_{90} show broad coarsening peaks in the first 24 h. As the milling process continues, the particles become harder, their tendency toward welding decreases, and the fracturing process predominates over the welding process, leading to a gradual decrease of the particle size. In time, a balance is achieved between welding and fracturing processes and the rate of decrease in size is decreased. The difference between d_{90} and d_{10} decreases with time and after 180 h attains a value of 16 to 18 μm for all
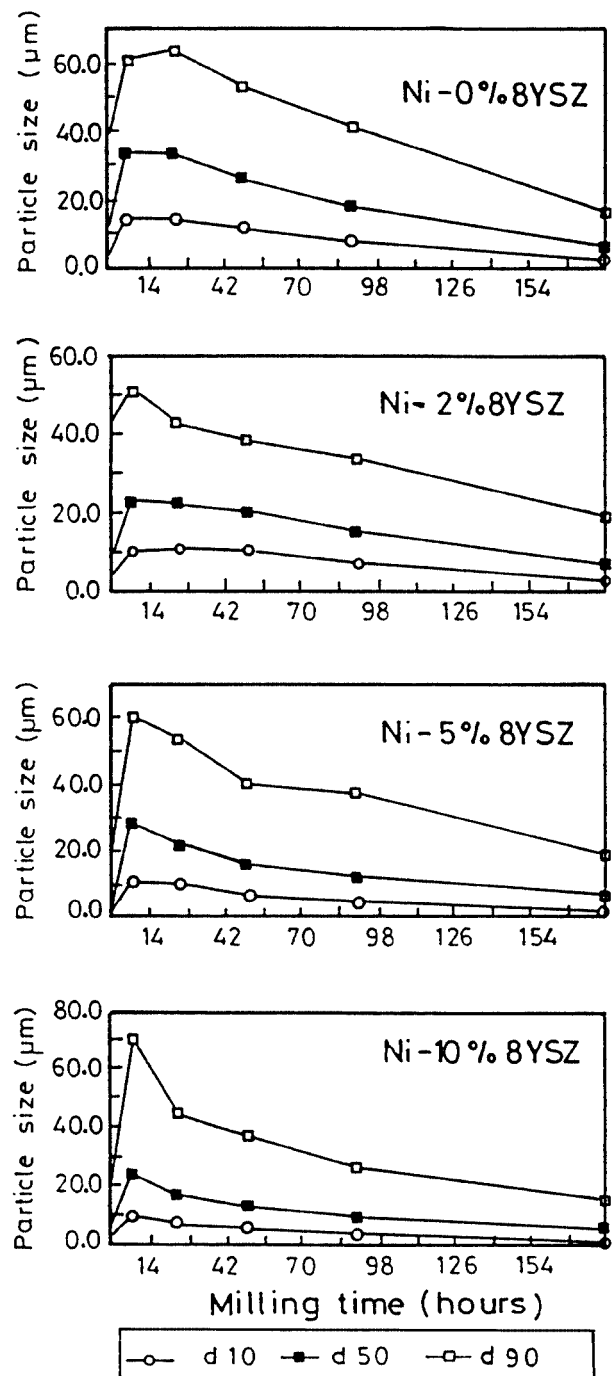

Fig. 1 Changes in different particle size fractions vs MA time for Ni powder with different volume fractions of 8YSZ

powders. This indicates more uniform distribution of the powder particle size after 180 h of milling.

Changes in the microstructure of the powder particles during MA have been extensively investigated by optical metallography at different MA stages. An example is shown in Fig. 2(a) to (d) for Ni-2% 8YSZ and Ni-10% 8YSZ powders. For both compositions, there is a slight decrease in the average particle size upon increasing the MA time from 90 to 180 h (Fig. 1 and 2). The noticeable difference, however, is that the
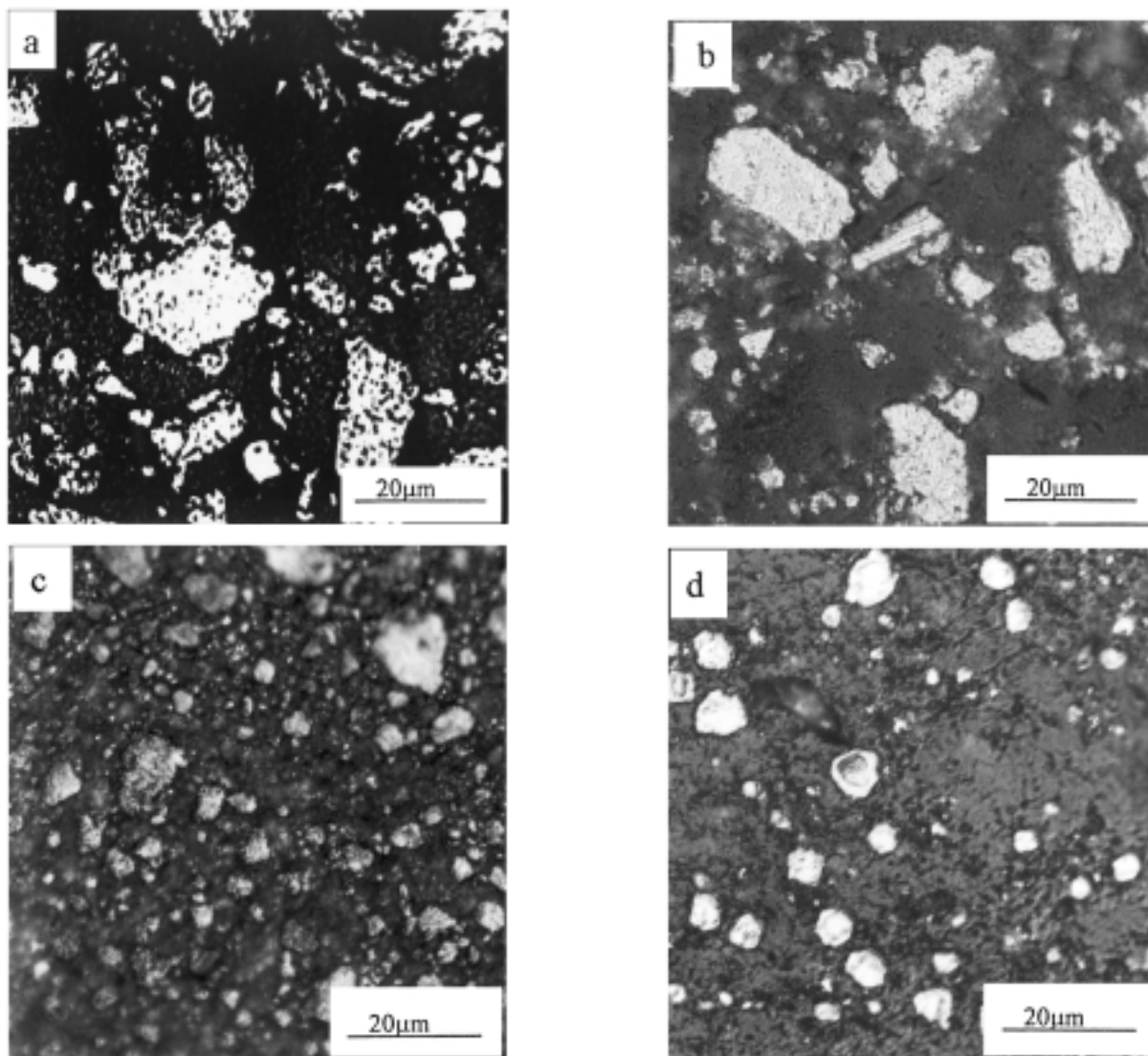
Fig. 2 Examples of the optical microstructure of etched sections for the mechanically alloyed powder mixtures: (**a**) and (**c**) Ni-2% 8YSZ and (**b**) and (**d**) Ni-10% 8YSZ. For (a, b) MA Time = 90 h, for (c, d) MA Time = 180 h

microstructure is continuously refined, where a featureless microstructure characteristic of complete MA is observed after 180 h compared to the layered structure observed after 90 h of milling (Fig. 2).

Figure 3(a) to (d) shows x-ray diffraction (XRD) patterns of Ni-8YSZ powder mixtures before and after MA for different time intervals. The just-blended powder of Ni and 8YSZ [curves 1 in Fig. 3(b) to (d)] exhibits an 8YSZ peak the intensity of which increases as its content is increased. The patterns of Fig. 3 show three distinct features. First, the 8YSZ peaks disappeared after MA for 180 h, a fact indicating that the 8YSZ has been deagglomerated and sufficiently dispersed in the matrix of Ni particles as a result of repeated welding and fracturing of the Ni particles and continued refinement of the structure. Second, NiO peaks could be detected after MA for 180 h, which indicates oxidation of some Ni during the MA process by the O_2 of the air atmosphere in the milling vials. Third, a significant reduction

in Ni peak intensities, as well as a considerable increase in the peak width compared to those of the just-blended powders, was observed. This can be attributed to high dislocation density in the particles, as they are subjected to extensive plastic deformation during the MA process. The overall peak broadening ΔK is composed of lattice strain broadening and crystallite size broadening[15,16,17] and is given by the equation

$$\Delta K = 0.9 \frac{2\pi}{(d)} + A \langle e^2 \rangle^{1/2} K \qquad \text{(Eq 1)}$$

where ΔK is the peak width at half-peak intensity; d is the crystallite size; A is a constant, which depends on the strain distribution and is approximately unity for uniform dislocation distribution; and $\langle e^2 \rangle^{1/2}$ is the relative lattice strain. The measured values of total width ΔK were corrected for instrumental broadening by subtracting 0.15° from their values and were substituted in Eq 1 to calculate d and $\langle e^2 \rangle^{1/2}$.
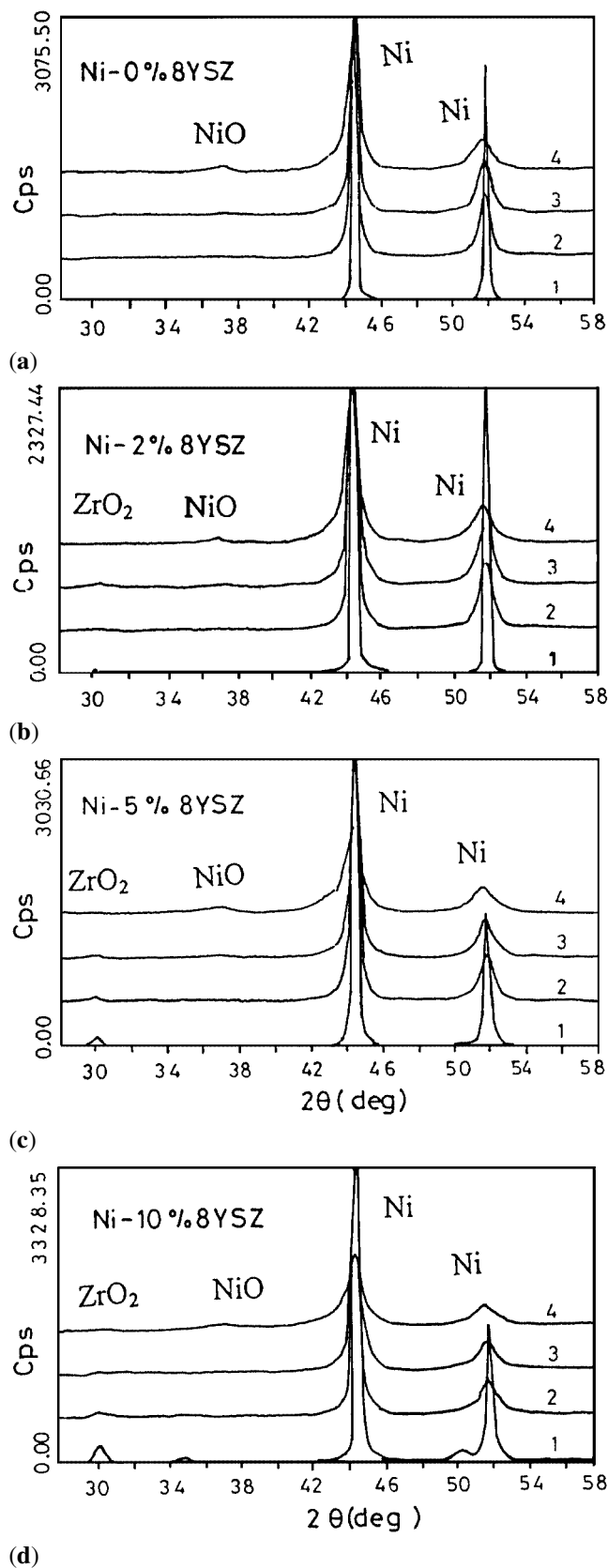
(a)

(b)

(c)

(d)

Fig. 3 (**a–d**) XRD patterns for different powder mixtures after different MA time intervals. For 1, 2, 3, and 4, MA time = 0, 50, 90, and 180 h
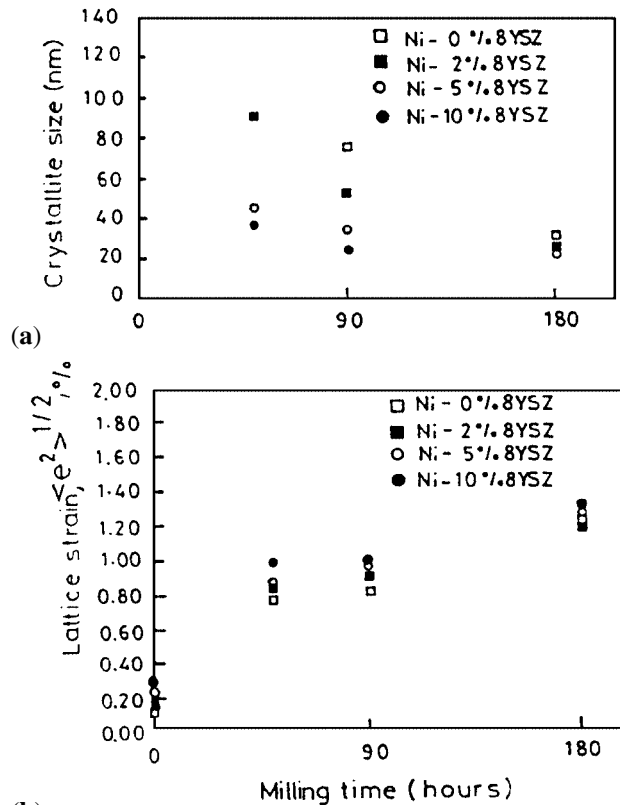

(a)

(b)

Fig. 4 Effect of MA time and 8YSZ content on the (**a**) crystallite size and (**b**) lattice strain

These values are plotted in Fig. 4(a) and (b) as a function of the milling time. The crystallite size decreases rapidly, while the lattice strain shows significant increase in the first 90 h of MA. The rate of refinement of crystallite size is higher for the higher contents of 8YSZ. The tendency for further refinement decreases gradually and a steady-state value is achieved after about 140 h for most of the powders treated. Increasing the MA time from 90 to 180 h decreased the crystallite size from 55 to 25 nm and from 30 to 23 nm for Ni-2% 8YSZ and Ni-5% 8YSZ, respectively. Nickel mechanically alloyed without additions of 8YSZ showed larger crystallite size, which decreased from 75 to 30 nm upon increasing the MA time from 90 to 180 h. On the other hand, the crystallite size of Ni-10% 8YSZ reached a steady-state value of 22 nm after 90 h of MA.

The lattice strain (Fig. 4b) increased rapidly in the first 90 h and then gradually afterwards, reaching a value of 1.3% for Ni-10% 8YSZ powder after 180 h. The other powder compositions exhibited similar behavior, but the values of strain are slightly lower. This rapid increase of strain in the first 90 h is corresponding to high rates of dislocation multiplication in the initial stages of plastic deformation during MA.[9,17]

3.2 Sintering and Microstructural Stability.

An example of the microstructure is given in Fig. 5(a) and (d) for the 180 h MA powder compacts after sintering for 1 h at 1100 °C. The figure shows very fine recrystallized grains
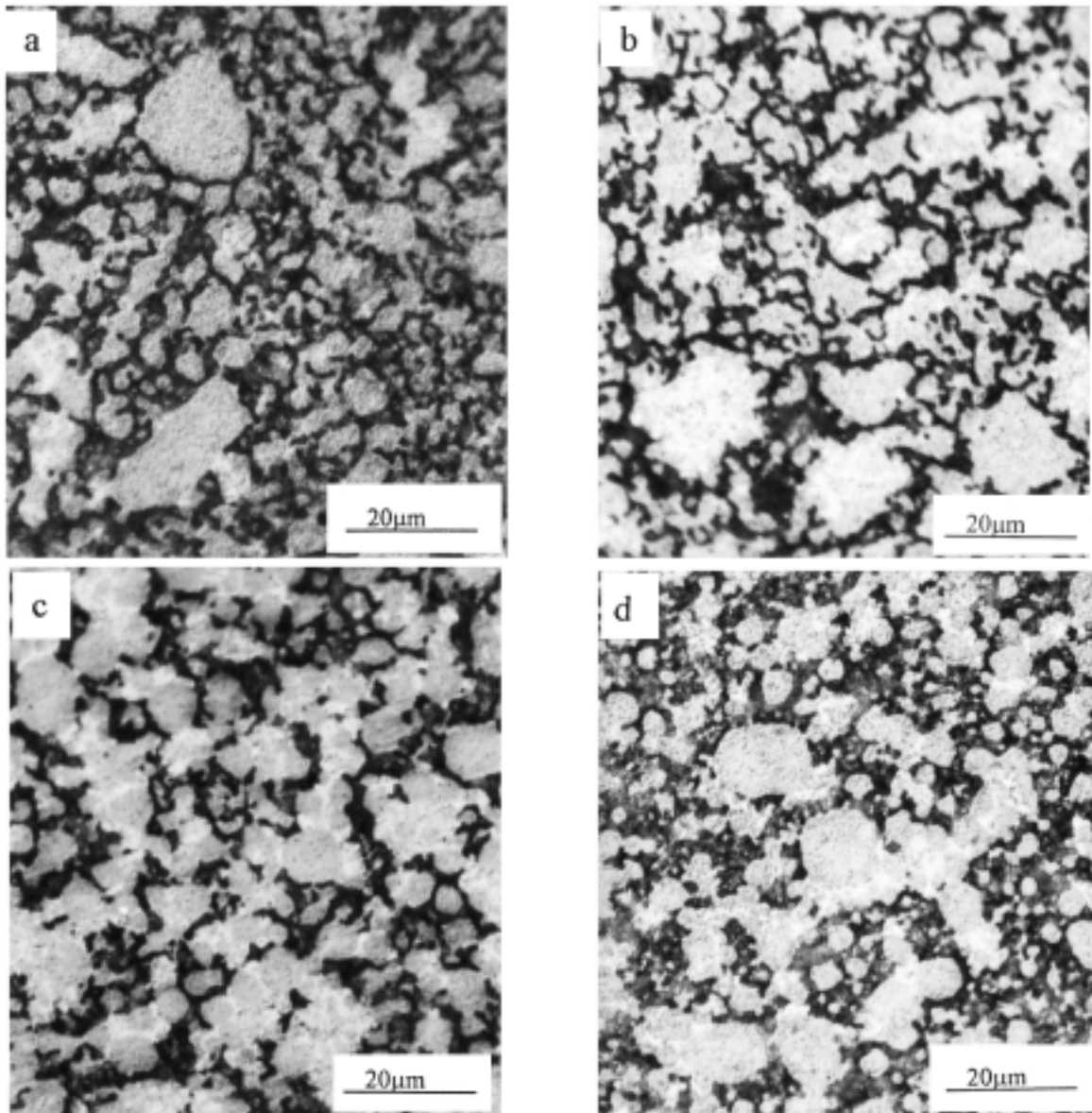
Fig. 5 Microstructure of 180 h mechanically alloyed powder compacts sintered for 1 h at 1100 °C: (**a**), (**b**), (**c**), and (**d**) Ni with 0, 2, 5, and 10% 8YSZ
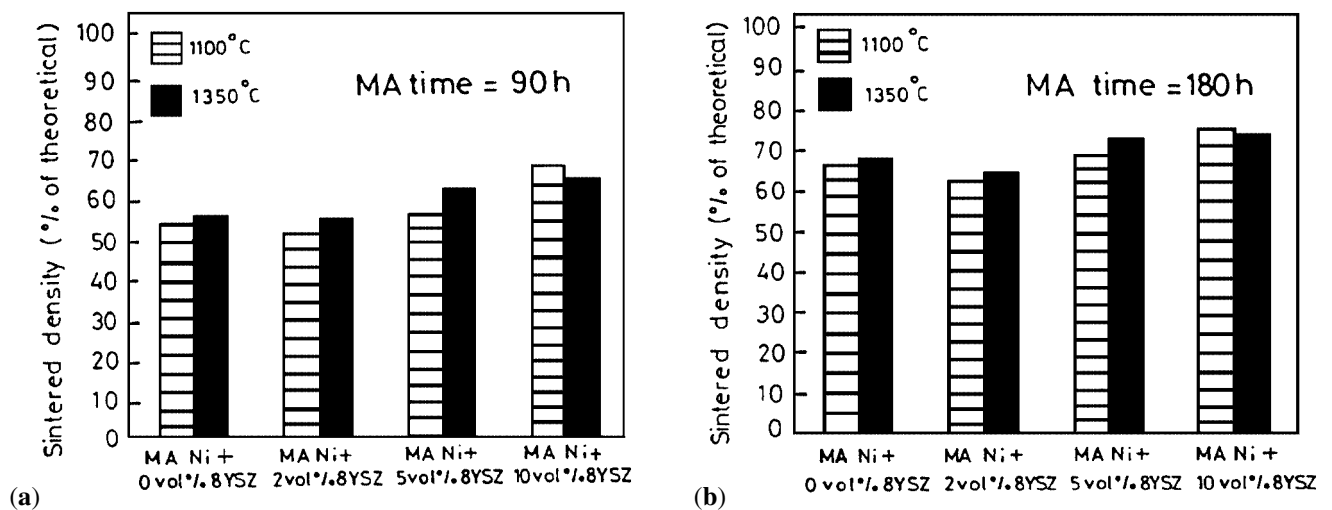

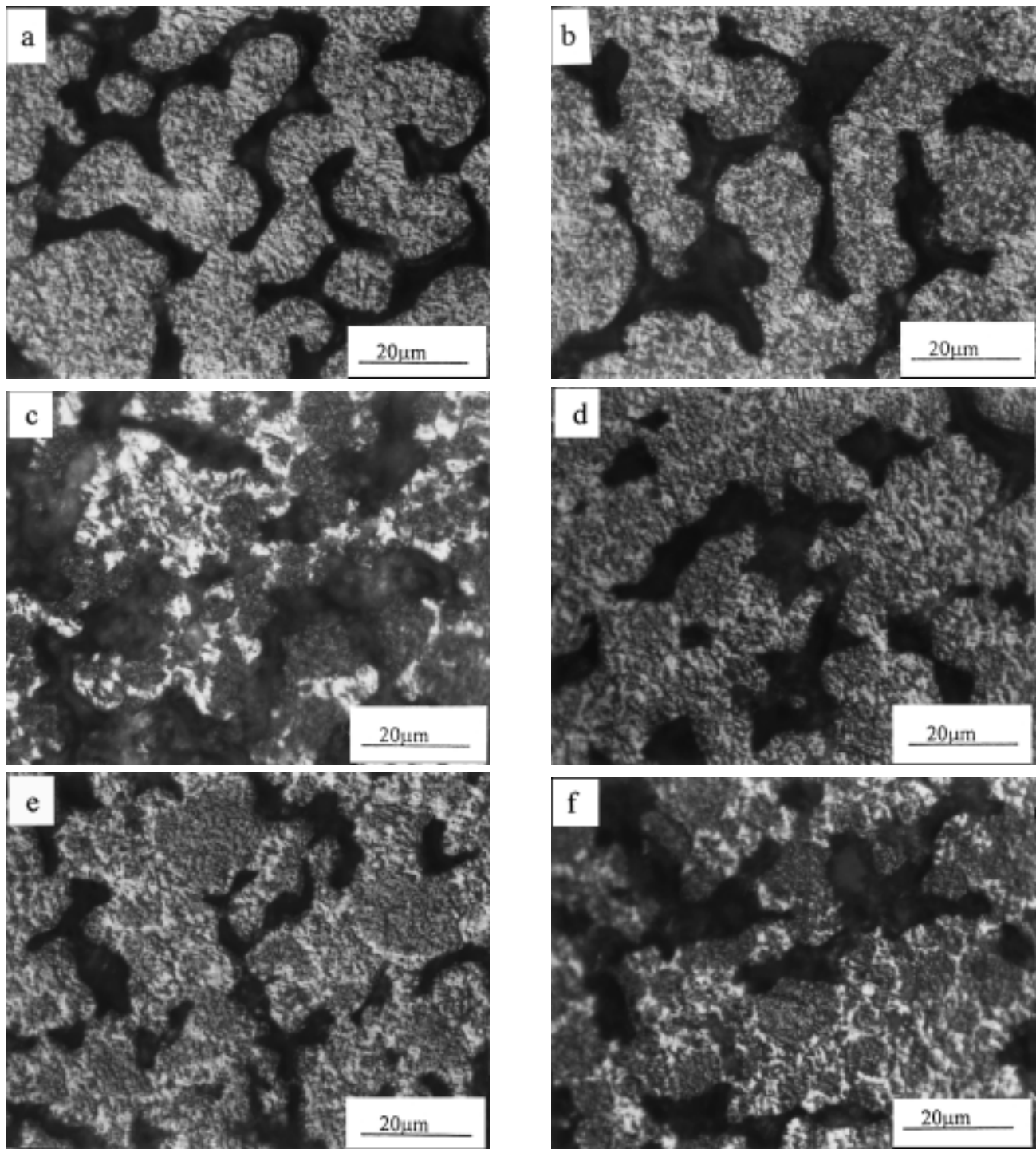**Fig. 6** (**a**) and (**b**) Effect of MA time, 8YSZ content, and sintering temperature on the sintered density of Ni-8YSZ compacts

Fig. 7 Microstructure of mechanically alloyed Ni-8YSZ compacts after sintering for 800 h at 1100 °C: (**a**) and (**d**) Ni-0% 8YSZ, (**b**) and (**e**) Ni-2% 8YSZ, and (**c**) and (**f**) Ni-10% 8YSZ. For (**a**) to (**c**), MA time = 90 h, and for (**d**) to (**f**), MA time = 180 h.

for the Ni-0% 8YSZ (Fig. 5a). Increasing the 8YSZ content seems to cause retardation of the recrystallization process. The corresponding loose powders showed featureless microstructures (Fig. 2). Figure 5(d) also shows formation of weld necks for the Ni-10% 8YSZ material. The relative density of the MA Ni-8YSZ powder compacts after sintering at 1100 and 1350 °C for 1 h is presented in Fig. 6. Unprocessed Ni samples sintered at 1100 and 1350 °C for 1 h achieved relative density of 84 and 89.5%, respectively. It is clear from Fig. 5 and 6 that MA of Ni with or without addition of 8YSZ inhibited the sintering process, with a maximum inhibition observed at about 2% 8YSZ. Increasing the sintering temperature from 1100 to 1350 °C did not cause considerable changes in densification, while increasing the MA time from 90 to 180 h increased the
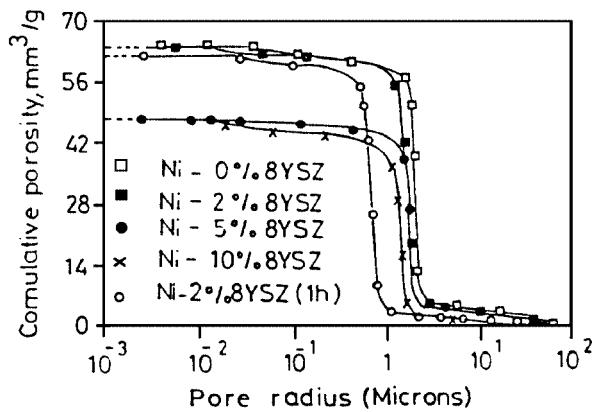
Fig. 8 Porosity distribution for 180 h mechanically alloyed powder compacts after sintering for 800 h at 1100 °C.

relative density by about 8 to 12%. This latter effect can be attributed to the increased fraction of the fine powder particles as the MA time was increased. Analysis of the particle size distribution showed that the volume fraction of the powder less than 3 μm in particle size is 7% after 90 h, while it increased to 20% after MA for 180 h for the Ni-10% 8YSZ powder mixture. These values were found to be 0 and 16% for the Ni-2% 8YSZ. Shrinkage during sintering is reported to be faster for the finer particle size powder.[18]

To study the microstructural stability samples of the MA Ni-8YSZ powder compacts were subjected to long-term sintering runs at 1100 °C. Figure 7(a) to (f) demonstrate the microstructural changes in these materials after sintering for 800 h. The Ni-0% and Ni-2% 8YSZ exhibit homogeneous microstructure with very fine grains (Fig. 7a, b, d, and e). The Ni-10% 8YSZ material showed inhomogeneous microstructure (Fig. 7c and f). A higher degree of inhomogenity is observed for the material mechanically alloyed for 90 h compared to that mechanically alloyed for 180 h. Energy-dispersive x-ray (EDX) analysis revealed that the gray areas (Fig. 7c) consist of Ni and 8YSZ, while the white areas are mainly Ni. It is evident from this figure that, after sintering for 800 h at 1100 °C, the materials mechanically alloyed for 90 or 180 h retain an interconnected porosity network with elongated pore morphology. This observation is supported by the results presented in Fig. 8, which shows the pore size distribution determined by the mercury porosimetry method dealing only with the open porosity of the material. It is clear from Fig. 8 that the material Ni-2% 8YSZ does not undergo remarkable changes in pore size distribution upon increasing the sintering time from 1 to 800 h. Correspondingly, the total porosity slightly decreased from 39.4 to 38.4%; however, the average pore size increased from 0.8 to about 2 μm. The Ni-0% 8YSZ showed nearly the same pore size distribution as that of Ni-2% 8YSZ, but the total porosity was found to be 36.4% compared to 38.4% for the Ni-2% 8YSZ. On the other hand, the materials containing 5 and 10% 8YSZ showed similar distribution (Fig. 8), but their specific porosity is considerably lower with respect to that of the Ni-0% or Ni-2% 8YSZ. The total porosity for the Ni-5% and Ni-10% 8YSZ is about 30.58% compared to 38.4% for the Ni-2% 8YS, reflecting higher sinterability for the materials containing higher amounts of 8YSZ after sintering at 1100 °C for 800 h. The total porosity

for a sample of unprocessed Ni powder compact was found to be 5% for the same sintering conditions.

The presented results clearly indicate that dispersion of fine 8YSZ by MA in Ni strongly hindered its densification during sintering throughout the entire range of 8YSZ investigated in this study. Maximum inhibition of sintering was noted at about 2% 8YSZ. Although an increase in densification after sintering of Ni-10% 8YSZ material is observed, the inhibiting effect still exists, since the relative density of this material is lower compared to that of unprocessed Ni under identical sintering conditions. Moreover, for the Ni-0% 8YSZ material, suppression of sintering was also noted (Fig. 5 to 8). In fact, after MA, this material is not oxide free. Chemical analysis of the mechanically alloyed powder of this material revealed that, after MA for 90 h, the material contained about 3.8 vol.% ZrO_2, and after MA for 180 h, the ZrO_2 content increased to about 5.5 vol.%. Similar amounts were also detected in the Ni powder mechanically alloyed with 8YSZ. The composite powder Ni-8YSZ, therefore, contains additionally 3.8 or 5.5 vol.% ZrO_2 depending on the MA time. Evidently, the source of ZrO_2 is the abrasion of the milling media due to ball-ball collision or to the impact of the balls with the wall of the milling containers.

Inhibition of sintering by dispersed particles is reported for numerous systems.[12,13] Particles were found to inhibit both the sintering mechanisms that cause neck growth and those that cause densification; however, it is the densifying mechanisms that are most profoundly affected.[12] The inhibited neck formation after sintering at 1100 °C for 1 h, particularly for the lower dispersoid content (Fig. 5), can be interpreted by suppression of plasticity through pinning of dislocations by the dispersed particles. The densifying mechanisms are largely affected by material flow during sintering. Interference of the dispersed particles, with the grain boundaries and free surfaces functioning as sources and sinks between which the material flows, causes suppression of the densifying mechanisms.[12] This inhibiting effect of the dispersoids remained effective after long-term sintering despite growth of large weld necks between nickel particles, as shown by Fig. 7 and 8. This observation is in agreement with the opinion that it is the densifying mechanisms that are strongly influenced by the dispersed particles. Retarded grain growth (Fig. 7a, b, d, and e) after sintering for 800 h can be attributed to pinning of the grain boundary dislocations by these particles.

Various metal/ceramic systems showed a minimum in sinterability with increasing dispersoid content.[12,19,20] The increase in sinterability after this minimum possibly implies that maximum stability of the dispersoid is reached and loss of coherency between the dispersoid particles and the metallic matrix takes place. This process enhances the sintering mechanisms and leads to agglomeration of the dispersed oxide particles. In the present work, the minimum in sinterability and the increase in densification observed for the Ni-10% 8YSZ samples are in agreement with the previous observations[12,19,20] and support the concept of agglomeration of dispersoid particles, as their concentration exceeds the minimum densification point. Loss of coherency and agglomeration process are expected to be more significant as the sintering time is increased at 1100 °C. Heterogenity of the microstructure of Ni-10% 8YSZ (Fig. 7c) after sintering for 800 h at 1100 °C may have resulted from the detachment of the 8YSZ particles from the Ni matrix after
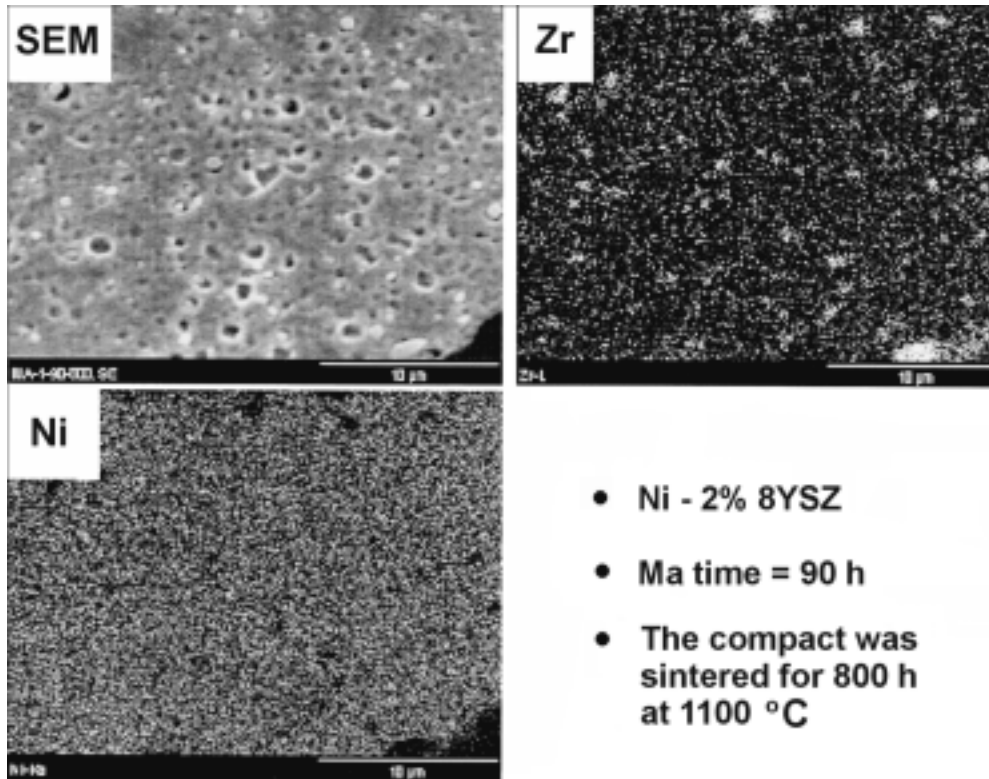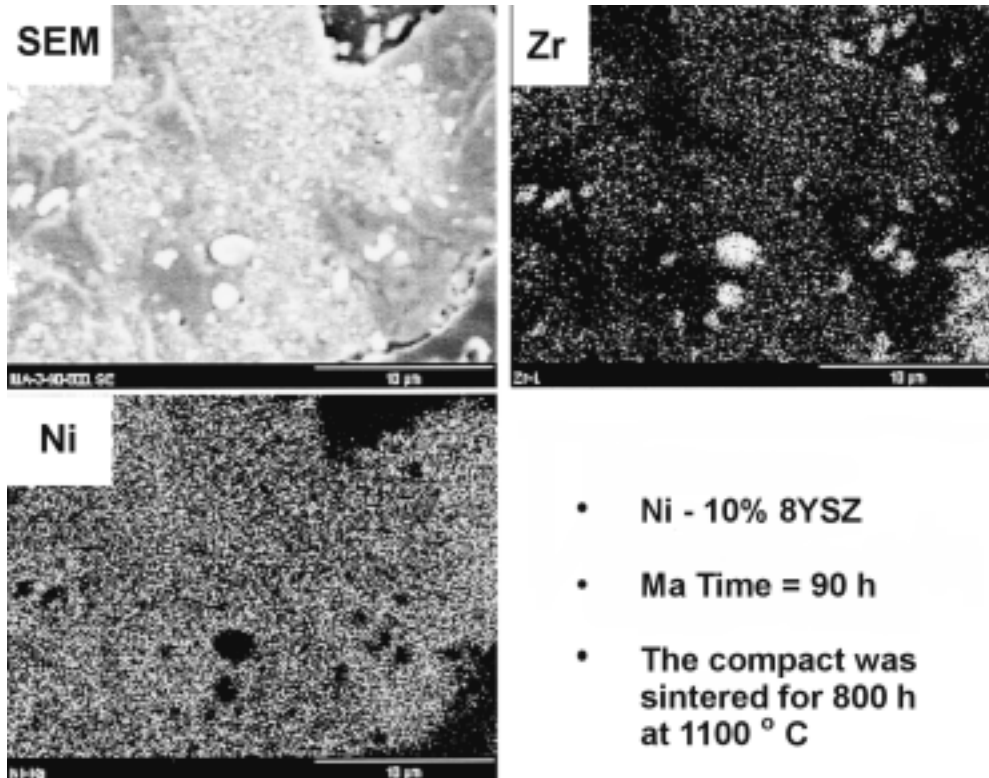
Fig. 9 SEM and EDX image of Zr and Ni for mechanically alloyed powder compacts after long-term sintering treatment. ● Ni-2% 8YSZ ● MA time = 90 h ● The compact was sintered for 800 h at 1100 °C ● Ni-10% 8YSZ ● MA time = 90 h ● The compact was sintered for 800 h at 1100 °C

this long sintering time. This leads to developing oxide-free areas and agglomeration of the detached fine oxide particles. Nonuniform distribution of Zr in this material is shown by the EDX image in Fig. 9(b). The composite powder compact containing 2% 8YSZ corresponding to a minimum in sinterability shows more uniform distribution of Zr (Fig. 9a) and very fine grains (Fig. 7b and d) after sintering for 800 h at 1100 °C, indicating long-term microstructural stability for this composition.

4. Conclusions

The composite powder Ni-8YSZ has been mechanically alloyed using high-energy ball milling in air atmosphere to produce oxide-dispersion strengthened nickel. Under the experimental conditions described in the present work, the following conclusions can be drawn.

- After 180 h of milling, the MA process is complete. The layered structure is no longer visible by optical microscopy. Peaks of 8YSZ disappeared from the XRD patterns and NiO peaks were observed. Additionally, the mechanically alloyed powder contains about 5.5 vol.% ZrO_2.

- The crystallite size and lattice distortion achieved their steady-state values after MA for about 140 h.

- Over the entire range of 8YSZ investigated, inhibited sintering of Ni was observed. Minimum sinterability was found at about 2% 8YSZ.

- The Ni-2% 8YSZ composite powder mechanically alloyed for 180 h showed considerable microstructural stability and retained sufficient porosity after extended sintering treatment in a reducing atmosphere.

References

1. R.C. Benn and P.K. Mirchandani: in "*New Materials by Mechanical Alloying Techniques,*" DGM Informationsgesellschaft Verlag, Oberursel, 1989, pp. 19-38.
2. J.S. Benjamin: *Sci. Am.,* 1976, vol. 234, pp. 40-48.
3. C.C. Koch: *Ann. Rev. Mater. Sci.,* 1989, vol. 19, pp. 121-143.
4. R. Orban and S. Domsa: "*Powder Metallurgy World Congress,*" PM 94, Paris, 1994, vol. 2, p. 1353.
5. O. Haruyama and N. Asahi: *J. Alloys and Compounds,* 1993, vol. 194, pp. 361-71.
6. C.C. Koch, O.B. Cavin, C.G. McKamey, and J.O. Scarbrough: *Appl. Phys. Lett.,* 1983, vol. 43, p. 1017.
7. J.S.C. Jang and C.C. Koch: *J. Mater. Res.,* 1990, vol. 5 (3), p. 498.
8. J. Eckert, L. Schultz, and K. Urban: *Appl. Phys. Lett.,* 1989, vol. 55, p. 117.
9. E. Hellstern, H.J. Fecht, Z. Fu, and W.L. Johnson: *J. Appl. Phys.,* 1989, vol. 65, p. 305.
10. D. Michel, F. Faudot, E. Gaffet, and L. Mazerolles: *J. Am. Cer. Soc.,* 1993, vol. 76 (11), p. 2884.
11. R. Wilkenhoener, T. Kloidt, and W. Mallener: in "*Electrochemical Proceedings,*" U. Stimming *et al.,* ed., The Electrochemical Society, Inc., Pennigton, NJ, 1997, p. 851.
12. M.F. Ashby, S. Bahk, J. Bevk, and D. Turnbull: *Progr. Mater. Sci.,* 1980, vol. 25, p. 1.
13. Y. Arami and O. Iwatsu: *J. Jpn. Soc. Powder Powder Metall.,* 1991, vol. 38, p. 47.
14. Y. Arami and O. Iwatsu: *J. Jpn. Soc. Powder Powder Metall.,* 1996, vol. 43, p. 1289.
15. A. Guiner: in "X-Ray Diffraction," W.H. Freeman, San Francisco, CA, 1963, p. 124.
16. J. Friedel: "*Dislocations,*" Pergamon Press, Oxford, United Kingdom, 1964, p. 418.
17. T.D. Shen, K.Y. Wang, M.X. Quan, and J.T. Wang: *J. Mater. Sci. Lett.,* 1992, vol. 11, p. 1570.
18. Y.H. Zhou, M. Harrmelin, and J. Bigot: *Scripta Metall.,* 1989, vol. 23, p. 1391.
19. M.H. Tikkanen, B.O. Rosell, and O. Wiberg: *Powder Metall.,* 1962, vol. 10, p. 49.
20. H. Scher and R. Zallen: *J. Chem. Phys.,* 1970, vol. 53, p. 759.